Simultaneous phase-shifting cyclic interferometer for generation of lateral and radial shear

D.I. Serrano-García[a], N.I. Toto-Arellano[a], A. Martínez García[a], J.A. Rayas Álvarez[a],
A. Téllez-Quiñones[a], and G. Rodríguez-Zurita[b]
[a]*Centro de Investigaciones en Óptica,*
A.C. Loma del Bosque 115 Col. Lomas del Campestre, 37150 Apartado Postal 1-948, León, Gto. México,
e-mails: david@cio.mx; ivantotoarellano@cio.mx
[b]*Facultad de Ciencias Físico-Matemáticas de la Benemérita Universidad Autónoma de Puebla,*
Apartado Postal 1152, Puebla, 72001, Pue., México.

Recibido el 4 de marzo de 2011; aceptado el 15 de abril de 2011

We present experimental results obtained by a phase-shifting interferometer employing polarization capable of retrieve directional derivatives in x-direction (lateral shear). The system was adapted to obtain radial derivative (radial shear) and implemented with a cyclic interferometer with phase grid to multiplex the interference patterns. Using phase shifting by polarization, the interferometer is capable of processing the optical phase data with n-interferograms captured in a single shot. Experimental results are presented.

Keywords: Diffraction; phase shifting; lateral shear; radial shear; interferometry; polarization.

En este trabajo se presentan los resultados experimentales obtenidos con un sistema interferométrico de corrimiento de fase por polarización, que puede obtener la derivada direccional en dirección x (desplazamiento lateral) y adaptando al arreglo para obtener la derivada radial (desplazamiento radial). El interferómetro que se presenta consiste de un interferómetro cíclico con rejilla de fase para multiplexar los patrones de interferencia. Usando las técnicas de corrimiento de fase por polarización, el interferómetro es capaz de procesar la fase óptica a partir de n-interferogramas capturados en una sola toma. Se presentan los resultados experimentales obtenidos.

Descriptores: Difracción; corrimiento de fase; desplazamiento lateral; desplazamiento radial; interferometría; polarización.

PACS: 42.87.Bg; 42.79.Ci; 42.79.Dj; 42.15.Eq; 42.25.Hz; 07.05.Pj

1. Introduction

In the lateral shearing interferometers the same wavefront is superposed with its copy but displaced a distance Δx. When Δx is sufficiently small, the phase difference can be approximated as the directional derivative of the wavefront in the displacement x-direction [1-2]. Due to this reason, it is sensitivity against high phase changes and the resultant interferograms are known as $shearograms$. Lateral shear interferograms have different fields of applications like optical tests, wavefront aberrations [3], phase singularities detection (optical vortex) [4], mechanical stress [5] among others. In the case of radial shear interferometers the superposition is against the same wavefront at different scales (contracted or expanded) with no displacement. In optical testing, the system is particulary sensitive at the astigmatism and coma aberrations and insensitive to defocus. The resultant patterns can be directly related to a Twyman-Green interferometer. The proposed system presents the advantage of obtain lateral and radial shear by using of the adequate components, both cases are studied and presented in this work.

2. Cyclic-Path interferometer

Figure 1 shows the interferometers proposed for lateral shear [6-8] and radial shear [9-13], the two optical systems are capable of obtain in a single shot n-shearograms with independent phase shifts [14-16]. Figure 1(a) shows the two possible interferometers that can be coupled to the 4-f system, each of them is used separately to generate a specified shear, the system-**I** is a Cyclic Shear Interferometer (CSI), where the shear is generated by moving the mirror M by a small distance $\triangle s$. The system-**II** is a cyclic radial shear interferometer (CRI), the optical setup is similar to the previously proposed, adding a pair of lens L_1 and L_2 to obtain the two beams with different diameter in the transversal section. In this case also lateral shear can be obtained only with a small displacement in M, resulting in a combination of a lateral and radial shear interferometer. Both systems are coupled to the 4-f system separately, each replica of the interference pattern obtained in the image plane, can be used to generate independent phase shift by placing linear polarizer filters in each replica. Figure 1(b) shows the plots representing the superposition of amplitude spectra in the output of the two systems.

2.1. Lateral shear interferometer

The system uses a laser source of He-Ne operating at $\lambda = 632.8$ nm. The collimated beam has a transversal section of $a = 8.6$ mm and linear polarization oriented to 45° generated by a quarter-wave retarder (Q_0) and a linear polarizer (P_0). The optical setup is a combination of a cyclic path interferometer and a 4-f system. In Fig. 1(a) the system-**I** represents the cyclic shear interferometer (CSI). By the use of a polarizing beam splitter (PBS) the resulting beams have

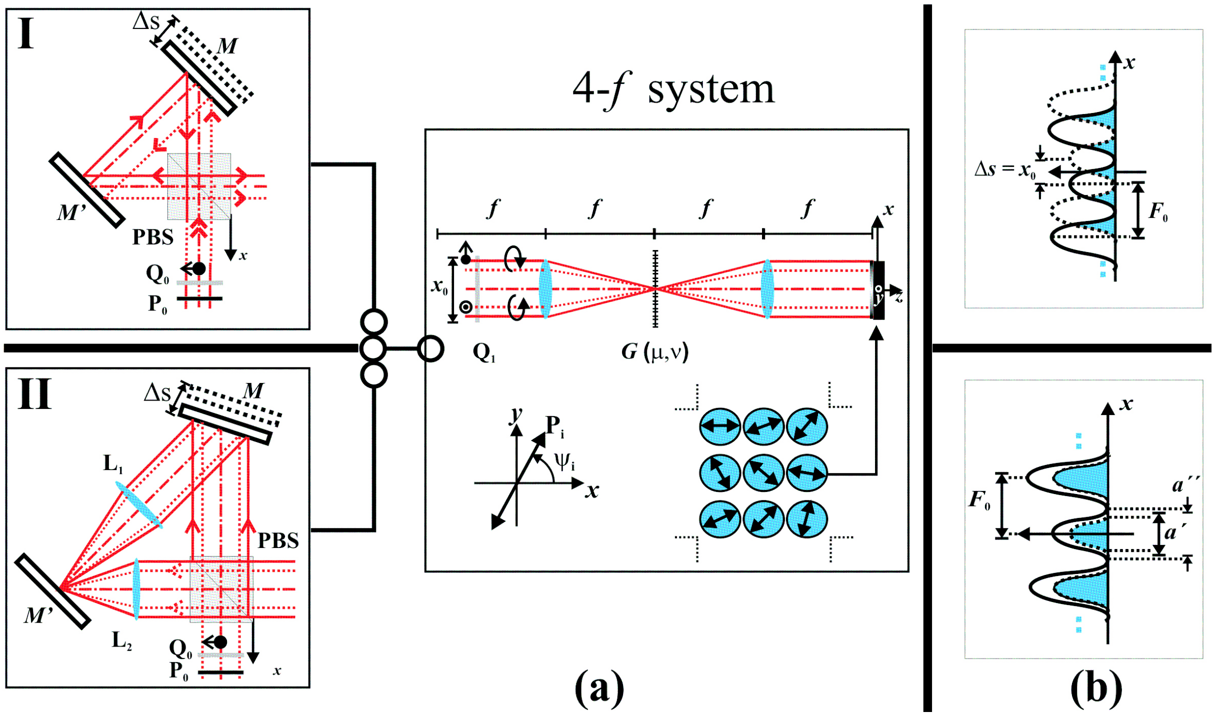

FIGURE 1. Shearing interferometers with phase grid and modulation of polarization. (a) Configuration **I** is a variable lateral-shear interferometer. The configuration **II** is a cyclic radial interferometer (CRI), which comprises a polarizing beam splitter (PBS), two lenses (L_1, L_2) and two mirrors (M, M'). Q_1: quarter-wave retarder; P_i: linear polarizers; ψ_i: transmission angle of polarization; Δs: linear shear; x_0: beam separation; F_0: order separation. (b) Upper row: diffraction orders of the same diffraction numerical order superimpose for lateral shear. Lower row: diffraction orders of different numerical order superimpose for radial shear.

cross linear polarization and after passing the quarter wave retarder (Q_1), right and left circular polarization is obtained. The mirrors used in the system are defined as M and M'. The 4-f system coupled to the cyclic interferometer uses two equals lenses ($f = 20$ cm) and a phase grid defined as $G(\mu, \nu)$ placed in the posterior focal plane of the first lens as the system's pupil with a spatial period d, where $\mu = u/\lambda f$ and $\nu = v/\lambda f$ are the frequency coordinates (u, v) scaled to the wavelength λ and the focal length f. Replicated beams of the interference pattern are obtained from this configuration. Placing a linear polarizer on each replica, an independent phase-shift can be obtained. No extra corrections were used in the angle of the linear polarizers used because the quarter wave retarders (Q_0, Q_1) operate at the wavelength of the source [14-15].

2.2. Replicated interference patterns and modulation by polarization

Defining the resultant vectorial beam amplitud of the CSI which enters to the 4-f system as

$$\vec{t}(x, y) = \vec{J}_L w\,(x, y) + \vec{J}_R w'\,(x + x_0, y)\,. \qquad (1)$$

where x_0 is the mutual separation of the beams along x, w is aperture of the reference beam and w' is the aperture of the beam sheared by distance x_0. $\vec{J}_R$ and $\vec{J}_L$ represents Jones vectors for right and left circular polarization as

$$\vec{J}_L = \begin{pmatrix} 1 \\ i \end{pmatrix}, \quad \vec{J}_R = \begin{pmatrix} 1 \\ -i \end{pmatrix}. \qquad (2)$$

The lateral shear of the wavefronts are adjusted by moving the mirror M of the CSI. The diagram in Fig. 1(a), system-**I** can be adjusted in such way that the lateral shear $\Delta s = x_0$ must be smaller than the transversal section **a** of the beams, this implies also that the lateral displacement is smaller than the diffraction order separation defined as F_0, see upper row of Fig. 1(b). The two mutually separated beams by a distance Δs enters to the 4-f system with cross linear polarization, after passing the quarter-wave retarder (Q_1) circular cross polarization are obtained. The phase grid is used to obtain replicated shearograms generated by the interferometric system (CSI). The replicated interference patterns can be modulated by polarization to obtain phase-shifts. The fringe pattern are defined as [15]:

$$I = 2J_q^2 J_r^2 \left\{1 + \cos[2\psi - \Delta\phi(x_q, y_r)]\right\} \qquad (3)$$

where ψ representing the angle of the linear polarizer,

$$x_q = x - qF_0, \quad y_r = x - rF_0,$$

$$\Delta\phi(x, y) = \phi(x, y) - \phi(x - x_0, y),$$

J_q and J_r are the Bessel function of order q and r respectively. The interference patterns presents unitary fringe modulation.

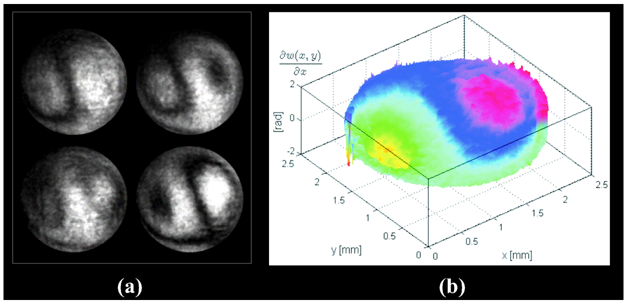

FIGURE 2. Typical interferograms for lateral shear obtained in a single shot (a) Interference patterns, (b) Unwrapped phase distributions of the interferograms sheared in x-direction.

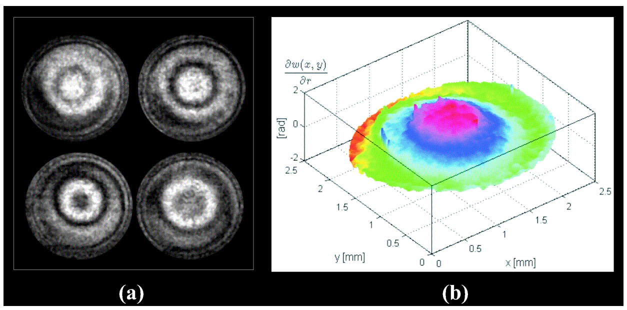

FIGURE 3. Typical interferograms for Radial shear obtained in a single shot. (a) Sheared interferograms of an aberrated wavefront. (b) Unwrapped phase distributions of the interferograms sheared in radial direction.

3. Radial shear interferometer

In Fig. 1(a), the system-**II** shows the optical arrangement used, where polarized light at 45° entering the interferometer generated by a quarter wave retarder (Q_0) and a linear polarizer (P_0). The cyclic radial interferometer (CRI) uses a polarizer beam splitter (PBS), two lens (L_1, L_2) and two mirrors (M, M'). Transversal sections of the beams can be described as:

$$w(x,y) = \text{circ}\left(\frac{\rho}{M_a}\right) \cdot e^{i\phi(x/M_a, y/M_a)},$$
$$w'(x,y) = \text{circ}(\rho) \cdot e^{i\phi(x,y)} \tag{4}$$

where $\rho = \sqrt{x^2+y^2}$ and $M_a = f_2/f_1$ denotes the relative magnification of the pupils as the focal lengths of both lenses (L_1,L_2). In the image plane of the 4-f system the fringe pattern obtained is modulated by the Bessel function as (3) but with radial symmetry, where

$$\Delta\phi(x,y) = \phi(x,y) - \phi(x/M_a, y/M_a).$$

As before in the lateral shear interferometer, at the image plane of the 4-f system replicated interference patterns that can be modulated by polarization are obtained with independent phase shifts.

4. Phase data processing

In general, the interference pattern can be described as [17]:

$$I_i(x,y) = A(x,y) + B(x,y)\cos\left[2\psi_i - \frac{\partial\phi(x,y)}{\partial x}\right], \tag{5}$$

for the case of lateral shear in x direction. $I_i(x,y)$ represents the $i = 1 \ldots 4$ intensity distribution captured by the CCD camera in a single shot, the polarization filters angles are: $\psi_1 = 0°$, $\psi_2 = 45°$, $\psi_3 = 90°$ and $\psi_4 = 135°$, each of them represent phase shifts of 0, $\pi/2$, π and $3/2\pi$ respectively. By considering that A and B are constant[15] the relative phase can be calculated as [18-19]:

$$\frac{\partial\phi(x,y)}{\partial x} = \arctan\left[\frac{I_1(x,y) - I_3(x,y)}{I_2(x,y) - I_4(x,y)}\right] \tag{6}$$

for the case of radial shear, Eq. (6) can be used only with the consideration of the radial dependency.

5. Experimental results with phase grid shearing interferometers

The experimental results presented in Fig. 2 and Fig. 3 were obtained by lens misalignments at defocus and paraxial focus respectively. Lateral shear interferograms representing spherical aberration with defocusing are shown in Fig. 2. The Fig. 2(a) presents the four patterns obtained simultaneously with relative shifts of $\pi/2$. Phase derivative in x-direction is presented in Fig. 2(b). A sets of n=4 typical experimental interferograms for radial shear are shown in Fig. 3(a) and the resulting unwrapped phase data in Fig. 3(b), representing a wavefront affected by spherical aberration in paraxial focus. Experimental results are presented for both cases of shear for an oil drop collocated on a microscope slide in Fig. 4 and Fig. 5, showing the capability of this system for measurement of surface deformations in fluids and also measurement of the concentration gradient profile of liquids. Figure 4(a) shows a typical sequence of four sheargrams obtained in single shot, and Fig. 4(b) shows the resulting unwrapped phase. Figure 5(a) shows sets of four experimental interferograms

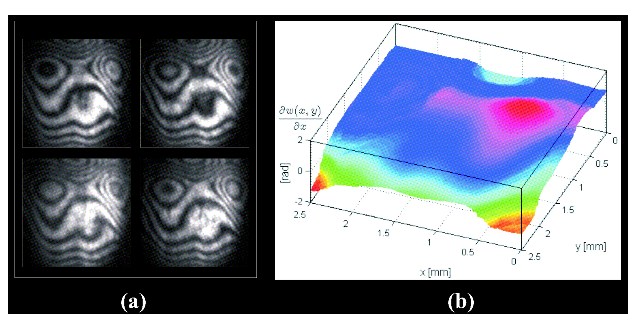

FIGURE 4. Static oil drop for the case of lateral shear. (a) Set of four sheargrams obtained in single shot. (b) Unwrapped phase showing the directional derivative.

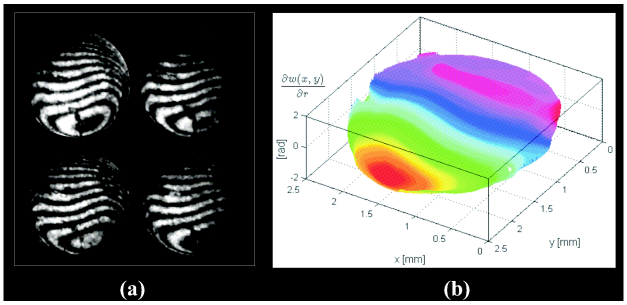

FIGURE 5. Static oil drop for the case of lateral and radial shearing combined. (a) Interference patterns with phase shifts of $\pi/2$. (b) Unwrapped phase distributions of the interferograms sheared in radial direction.

obtained combining linear shear and radial shear and 5(b) the resulting unwrapped phase. Experimental results are presented using four interference patterns to retrieve the optical phase data using the four steps algorithm [20-21]. Each of the interferograms was subjected to the same scaling (0-255 gray levels) and low-pass filtering process before phase calculation.

6. Conclusions

A cyclic path shearing interferometer coupled to a 4-f system with a phase grid, to achieve simultaneously n-shearograms for phase measurement by phase-shifting techniques has been implemented for the case of lateral and radial shear. The system presented can use other grating types but the irradiance ratios, fringe modulation values and polarization distribution changes. The system is mechanically stable against external vibration and can be used in beam characterization, microscopy, tomography, holography, phase slope measurement or optical testing.

Acknowledgements

One of the authors (NITA) occupies a second year to postdoctoral research position at CIO and expresses sincere appreciation to Luisa, Miguel, and Damian for the support provided, and to CONACYT for grant 102137/43055. Partial support from El Consejo Nacional de Ciencia y Tecnologia (CONACYT) and Centro de Investigaciones en Óptica A.C. (CIO) through projects 290597 (CONACYT-CIO) and 124145 (CONACYT-BUAP) is also acknowledged. The author DISG (Grant:227470/31458) is very grateful to CONACyT for the graduate scholarship granted and expresses sincere appreciation to Geliztle. ATQ is grateful to CONACYT for financial support through scholarship 227470/31458.

1. M.V. Mantravadi, *Lateral shearing interferometers* 2nd ed. (D. Malacara, ed. Wiley, New York, 1992).
2. M.V. Murty, *Appl. Opt.* **12** (1973) 2765.
3. K. Mastuda, Y. Minami and T. Eiju, *Appl. Opt.* **31** (1992) 6603.
4. D. Pal Ghai, S. Vyas, P. Senthilkumaran, and R.S. Sirohi, *Optics and Lasers in Engineering* **46** (2008) 419.
5. K. Patorski, *Appl. Opt.* **27** (1988) 3567 .
6. D. Malacara, *c.4 in Optical Shop Testing* 3nd ed. (D. Malacara, ed. Wiley, New York, 2007).
7. T. Kreis, *J. Opt. Soc. Am. A* **3** (1986) 847.
8. A. Cornejo-Rodriguez, *Ronchi test, c.9 in Optical Shop Testing* 3nd ed., (D. Malacara, ed. Wiley,New York, 2007).
9. P. Hariharan and D. Sen, *J. Sci. Instrum.* **37** (1960) 374.
10. R.F. Horton, *Opt. Engineer.* **27** (1988) 1063.
11. D. Malacara, *Appl. Opt.* **13** (1974) 1781.
12. M.V. Murty, *Appl. Opt.* **3** (1964) 853.
13. R.F. Horton, *Opt. Engineer.* **27** (1988) 1063.
14. G. Rodríguez-Zurita, C. Meneses-Fabian, N. Toto-Arellano, J.F. Vázquez-Castillo, and C. Robledo-Sánchez, *Opt. Express* **16** (2008) 7806.
15. N. Toto-Arellano, G. Rodríguez-Zurita, C. Meneses-Fabian, and J.F. Vázquez-Castillo, *Opt. Express* **16** (2008) 19330.
16. G. Rodríguez-Zurita, N. Toto Arellano, C. Meneses-Fabian, and J. Vazquez-Castillo, *Opt. Letters* **33** (2008) 2788.
17. N.I. Toto-Arellano, A. Martínez-García, G. Rodríguez-Zurita, J.A. Rayas-Álvarez, and A. Montes-Perez, *Appl. Opt.* **49** (2010) 6402.
18. D.K. Sharma, R.S. Sirohi, and M.P. Kothiyal, *Appl. Opt.* **23** (1984) 1542.
19. B. Barrientos-García, A.J. Moore, C. Pérez-López, L. Wang, and T. Tschudi, *Appl. Opt.* **38** (1999) 5944.
20. B. Barrientos-García, A.J. Moore, C. Pérez-López, L. Wang, and T. Tschudi, *Opt. Eng.* **38** (1999) 2069.
21. D. Malacara, M. Servin, and Z. Malacara, *c.6 in Phase detection algorithms in Interferogram Analysis for Optical Testing* (Marcel Dekker, New York 1998).